MATIGNON, C. & DELEPINE, M. (1901). *C.R. Acad. Sci., Paris*, **132**, 36.
PAULING, L. (1947). *J. Amer. Chem. Soc.* **69**, 542.
PAULING, L. & EWING, F. J. (1948). *J. Amer. Chem. Soc.* **70**, 1660.
RUNDLE, R. E. (1947). *J. Amer. Chem. Soc.* **69**, 1719.
RUNDLE, R. E. (1951). *J. Amer. Chem. Soc.* **73**, 4172.
SHULL, C. G. & WOLLAN, E. O. (1951). *Phys. Rev.* **81**, 527.
SIEVERTS, A. & ROELL, E. (1926). *Z. anorg. Chem.* **153**, 299.
SPEDDING, F. J., NEWTON, A., WARF, J., JOHNSON, O., NOTTORF, R., JOHNS, I. & DAANE, A. (1949). *Nucleonics*, **4**, 4.
STACKELBERG, M. VON (1930). *Z. phys. Chem.* (B), **9**, 437.
WINKLER, C. (1891). *Ber. dtsch. chem. Ges.* **24**, 886.
WOLLAN, E. O. & SHULL, C. G. (1948). *Phys. Rev.* **73**, 830.
ZACHARIASEN, W. H. (1944). *Manhattan Project Report*, CC–2166.

Acta Cryst. (1952). **5**, 26

The Crystal Structure of Tricalcium Silicate*

BY J. W. JEFFERY

Birkbeck College Research Laboratory, 21 Torrington Square, London W.C. 1, England

(*Received 27 September 1950 and in revised form 25 April 1951*)

Three polymorphic forms of tricalcium silicate, $3CaO.SiO_2$, the most important constituent of Portland cement clinker, have been studied. All three are strongly pseudo-rhombohedral, with hexagonal axes $a=7{\cdot}0$, $c=25{\cdot}0$ Å approximately. The pseudo-structure, which is a good approximation to the true structures of all three forms, has been determined. The space group is $R3m$ and $Z=9$ for the hexagonal cell. The true symmetry, cell size and space group have been determined for the form known as alite, which has a composition $54CaO.16SiO_2.Al_2O_3.MgO$, i.e. in 18 molecules of $3CaO.SiO_2$, two silicon atoms have been replaced by aluminium, with one magnesium atom entering the structure to balance the charges. This form is monoclinic, Cm, with

$$a=33{\cdot}08, \quad b=7{\cdot}07, \quad c=18{\cdot}56 \text{ Å}, \quad \beta=94^\circ\ 10',$$

and has two 'molecules' per unit cell.

Some preliminary deductions are made about the position of the aluminium and magnesium atoms in the unit cell and also about the type of distortion of the pseudo-structure which would account for the diffraction effects.

Introduction

The importance of tricalcium silicate, $3CaO.SiO_2$, arises from its occurrence in Portland cement. The main cementing material found in Portland cement clinker was called 'alite' by Tornebohm, who, with Le Chatelier, laid the basis for the modern theories of the composition of cement clinker. This occurred towards the end of the last century, and the problem of the composition and structure of alite has been the subject of controversy and speculation up to the present time.

A critical review of pre-war work has been given by Jeffery (1950), together with results obtained during the course of the present investigation. The accumulated evidence shows that alite is tricalcium silicate modified by slight 'solid solution'.

Polymorphism of tricalcium silicate

At least three forms of tricalcium silicate have been shown to exist. All three give, on rotation photographs with normal exposures, almost identical patterns, typified by the strong reflexions of Fig. 1, with row lines indicating rhombohedral symmetry. Laue photographs along the c axis (Fig. 2) also show the pseudo-trigonal character of all three forms. The approximate pseudo-hexagonal cell dimensions are

$$a=7{\cdot}0, \quad c=25{\cdot}0 \text{ Å}.$$

On rotation photographs with long exposures the lack of complete rhombohedral symmetry is shown by the complex character of high-angle reflexions and the occurrence of 'extra' reflexions. All three forms show these effects, but in different ways.

The characteristics of the three forms of tricalcium silicate which have been investigated

(*a*) *Pure tricalcium silicate*

The rotation photograph (Fig. 3) and the Laue photograph along the pseudo-hexagonal c axis (Fig. 2) show that this form is triclinic, with three unequal pseudo-hexagonal a axes. Powder photographs show many doublets where the other forms give single lines. The most clearly resolved doublet occurs at $d=1{\cdot}466$

* This paper is an abridged and amended version of part of a thesis approved by the University of London for the degree of Ph.D.

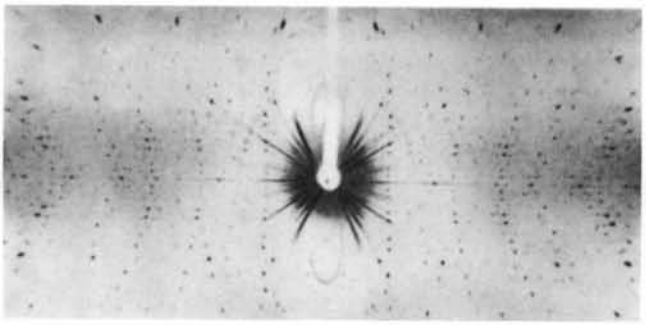

Fig. 1. Rotation photograph of alite about c. Cu $K\alpha$ radiation; 62 hr. exposure; 20 mA.; 40 kV.P.

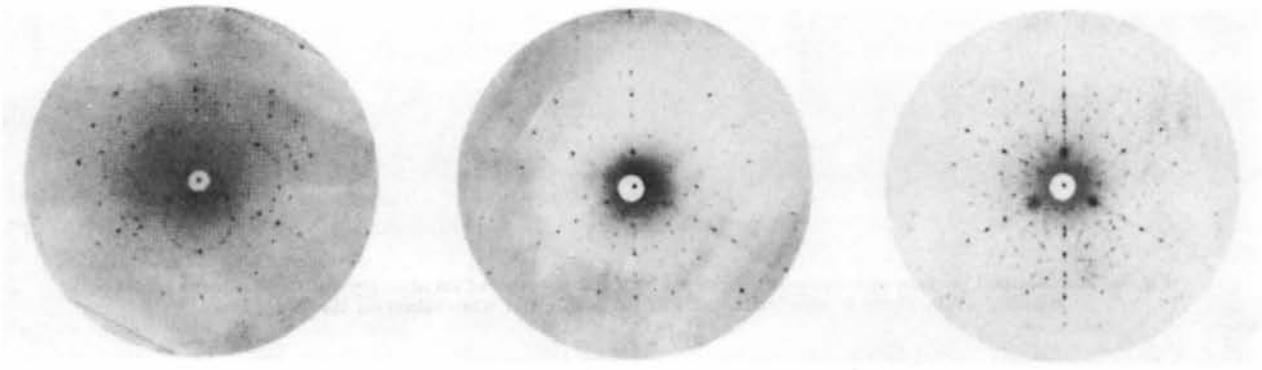

(*a*) (*b*) (*c*)

Fig. 2. Laue photographs with the beam along the c axis. (*a*) Pure tricalcium silicate. (*b*) Material isolated from slag. (*c*) Alite.

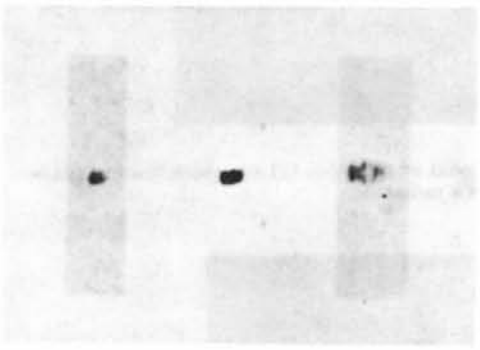

(*a*) (*b*) (*c*)

Fig. 3. Enlarged portions of rotation photographs about c, showing 4480. Cu $K\alpha$ radiation. (*a*) Slag. (*b*) Alite. (*c*) Pure tricalcium silicate.

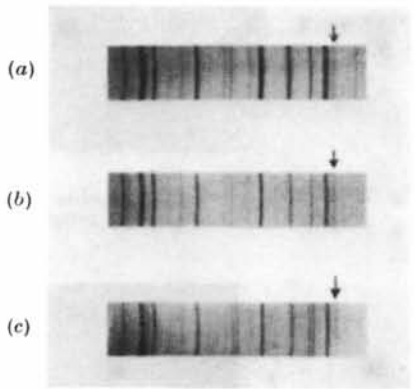

Fig. 4. Low- to medium-angle portions of 19 cm. powder photographs. Cu $K\alpha$ radiation. (*a*) Pure tricalcium silicate. (*b*) Recrystallized alite. (*c*) Cement clinker, showing lines due to tricalcium aluminate as well as alite.

[*To face p.* 26

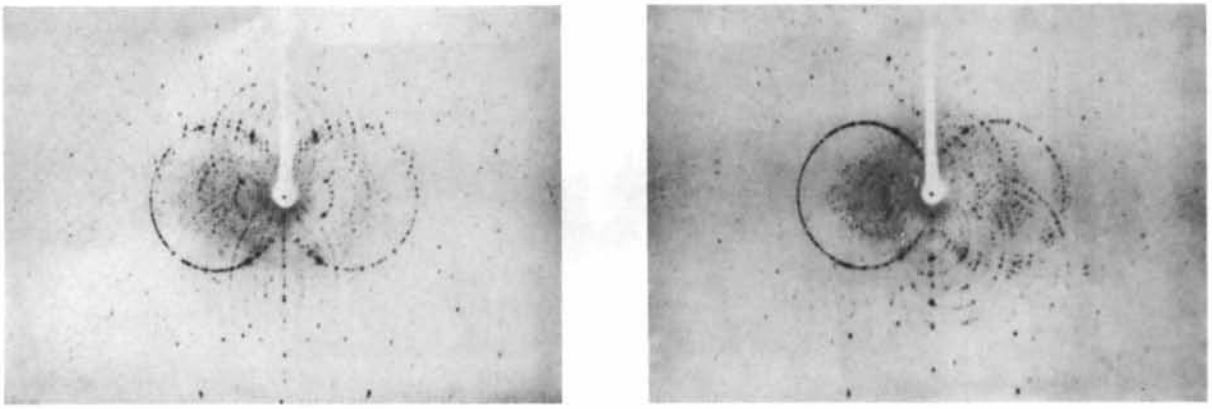

(*a*) (*b*)

Fig. 5. Laue photographs of alite with the beam perpendicular to the *c* axis. (*a*) Beam in the reflexion plane. (*b*) Beam in the pseudo reflexion plane.

Fig. 6. An enlarged portion of a composite Weissenberg photograph of an alite crystal from cement clinker, showing 4480. Three 5° oscillations at 120° to each other were taken on the same film.

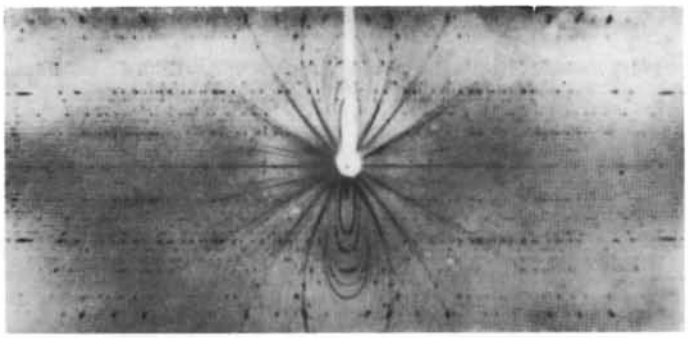

Fig. 7. Rotation photograph of alite about the hexagonal a^* direction [21.0], which lies in the true reflexion plane. Cu $K\alpha$ radiation.

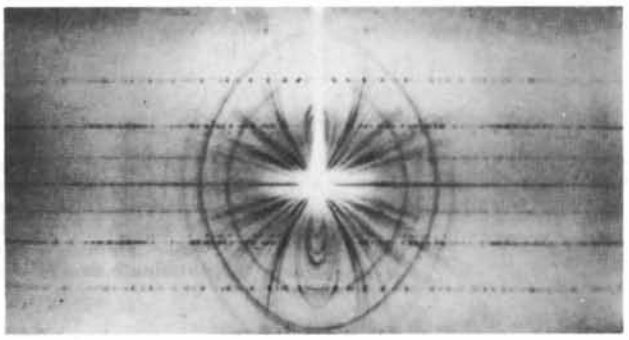

Fig. 8. Rotation photograph of alite about the monoclinic *b* axis. Cu $K\alpha$ radiation.

and 1·454 Å and is indicated by an arrow in Fig. 4. However, because one of the strong lines of CaO ($d=1·447$ Å) is very near to this doublet, it may be better to rely for identification in mixtures which may contain CaO on the stronger but less well-resolved doublets at $d=1·497$, 1·481 and 1·771, 1·752 Å.

The single crystals of this form appear to be paramorphs of a high-temperature form which probably has a true rhombohedral lattice (Jeffery, 1950).

(*b*) *Tricalcium silicate crystallized from basic slag*

This form contains small quantities of FeO, Fe_2O_3, MnO and P_2O_5, as well as MgO and Al_2O_3. The Laue and rotation photographs (Figs. 2, 3) show that it is extremely similar to form (*c*), the only difference detectable in the rather small crystals so far available being the absence of splitting of the high-angle reflexions.

Guttmann & Gille (1933*a*, *b*) investigated crystals from the same source and concluded that they were either trigonal or very strongly pseudo-trigonal, with hexagonal cell dimensions in agreement with those given above.

(*c*) *Alite–tricalcium silicate containing small amounts of* MgO *and* Al_2O_3

The rotation photographs (Figs. 1, 3) and the Laue photographs (Figs. 2, 5) show that this form is monoclinic. It was at first thought (Jeffery, 1950) that the splitting into triplets (on rotation photographs) of $44\bar{8}0$ and other high-angle reflexions was due to the unique pseudo-hexagonal a axis ($\equiv b$) being slightly shorter than the other two. However, the composite Weissenberg photograph (Fig. 6) shows that each reflexion has this triple character. The axes are therefore presumably of equal length, but the splitting is clearly a complicated effect (some pseudo-rhombohedral reflexions are split into four while the 'extra' reflexions are normal doublets), and its precise significance remains to be investigated. The inner reflexion of the triplet was used for calculating cell dimensions.

Alite gives a number of single lines on powder photographs corresponding to doublets given by pure tricalcium silicate. The most characteristic line in this respect has $d=1·457$ Å and is shown by an arrow in Fig. 4. The lines corresponding to the other doublets given for pure tricalcium silicate have $d=1·485$ and 1·761 Å.

There is less suggestion of paramorphism in the crystals of this form, and it is possible that there is no transition to a higher symmetry at high temperatures.

Materials

Large crystals of pure tricalcium silicate and alite for use in this investigation were made by Nurse (1949) at the Building Research Station. Small crystals of alite were obtained from clinker which had been formed at a high temperature. Small crystals of tricalcium silicate from open-hearth furnace slag were obtained, through the courtesy of Prof. Tilley, from a piece of the same slag that Andersen & Lee (1933) and Guttmann & Gille (1933*a*, *b*) used in their investigations.

The identity of rotation and powder photographs showed that the large crystals of alite (recrystallized from molten $CaCl_2$) had the same structure as the crystals obtained direct from the clinker, although 'extra' reflexions were not visible at high angles in the much weaker clinker photograph.

Determination of the pseudo-structure

(*a*) *General*

In the first stage of the investigation the departure from rhombohedral symmetry was neglected, and a pseudo-structure which is a good approximation to all the true structures was determined.

The data for this part of the work were taken from multiple-film rotation and Weissenberg photographs of the recrystallized alite. This was occasionally supplemented, in some of the cases where reflexions from different crystallographic forms coincided on the rotation photographs, by the use of oscillation photographs of slag and pure tricalcium silicate crystals. Rough intensity estimations for almost the whole diffraction pattern are given in Table 1 *without correction* for the Lorentz and polarization factors.

Hexagonal axes and indices have been used throughout the paper.

(*b*) *Special features of the diffraction pattern*

(i) All reflexions with h or k odd are weak or missing. This pseudo-halving of a is particularly noticeable in the higher-angle reflexions.

(ii) In the $hh\bar{2}\bar{h}l$ zone, besides the pseudo-halving of a, reflexions are present only for $l=9n$, indicating thirding of the rhombohedral layer in this projection. The exceptions, which are very weak, occur in the $11\bar{2}l$ row line at small θ values and at larger θ values in some $000l$ reflexions. However, 0003 and 0006 are completely absent.

(iii) In the $hki0$ zone the pseudo-halving of a is almost exact, the only exception being $33\bar{6}0$ (w).

(iv) For $60\bar{6}l$, reflexions are present only for $l=9n$.

(*c*) *Crystal class*

The optical goniometrical results (Andersen & Lee, 1933; Guttmann & Gille, 1933*a*, *b*) are compatible with the crystal classes $\bar{3}m$, $3m$, 32, as is the diffraction symmetry. Only the first class has a centre of symmetry.

The liquid-air test for pyro- or piezo-electricity and a test for piezo-electricity on a sensitive Giebe–Scheibe apparatus both gave negative results. Wooster (1949, p. 217) states that salts containing radicals of tetrahedral form are generally not piezo-electric. In tricalcium silicate it is almost certain that SiO_4 tetrahedra occur as separate radicals, and this, rather than

Table 1. *Intensities*

h0$\bar{h}$l

l	*h*=3	*h*=6	*l*	*h*=1	*h*=4	*h*=7	*l*	*h*=2	*h*=5	*h*=8
18	*a**	*w**	20	—	*a*	*a*	19	*w*	*a*	*a*
15	*vw**	*a**	17	—	*vvw*	*a*	16	*vw*	*a*	*a*
12	*w*	*a*	14	*a*	*m*	*vvw*	13	*vs*	*a*	*vvw*
9	*w*	*s*	11	*a*	*vvw*	*a*	10	*s*	*a*	*a*
6	*w*	*a*	8	*a*	*w*	*a*	7	*s*	*a*	*a*
3	*m*	*a*	5	*vw*	*s*	*vw*	4	*vs*	*a*	*vvw*
0	*vvw*	*s*	2	*a*	*vw*	*a*	1	*vs*	*a*	*a*
$\bar{3}$	*m*	*a*	$\bar{1}$	*vvw*	*w*	*a*	$\bar{2}$	*m*	*a*	*a*
$\bar{6}$	*w*	*a*	$\bar{4}$	*a*	*s*	*vw*	$\bar{5}$	*vs*	*a*	*vvw*
$\bar{9}$	*w*	*m*	$\bar{7}$	*a*	*vw*	*a*	$\bar{8}$	*vs*	*a*	*a*
$\bar{12}$	*w*	*a*	$\bar{10}$	*vvw*	*vw*	*a*	$\bar{11}$	*w*	*a*	*a*
			$\bar{13}$	*a*	*m*	*vvw*	$\bar{14}$	*vs*	*a*	*vvw*
			$\bar{16}$	—	*a*	*a*	$\bar{17}$	*w*	*a*	*a*
			$\bar{19}$	—	*a*	*a*	$\bar{20}$	*vvw*	*a*	*a*

h.h.$\bar{2}$$\bar{h}$.l ($\bar{l}$=*l*)

l	*h*=0	*h*=1	*h*=2	*h*=3	*h*=4	*h*=5
30	*vvw*	—	—	—	—	—
27	*s*	—	*w*	*a*	*a*	*a*
24	*a*	—	*a*	*a*	*a*	*a*
21	*vvw*	*a*	*a*	*a*	*a*	*a*
18	*vs*	*a*	*vs*	*a*	*vw*	*a*
15	*vvw*	*vvw*	*a*	*a*	*a*	*a*
12	*vvw*	*vvw*	*a*	*a*	*a*	*a*
9	*vvs*	*s*	*vs*	*a*	*w*	*a*
6	*a*	*w*	*a*	*a*	*a*	*a*
3	*a*	*vvw*	*a*	*a*	*a*	*a*
0	—	*w*	*vvs*	*w*	*m*	*vvw*

hkil

l	*hki*= 21$\bar{3}$	*hki*= 32$\bar{5}$	*hki*= 51$\bar{6}$	*hki*= 43$\bar{7}$	*hki*= 62$\bar{8}$	*hki*= 54$\bar{9}$	*l*	*hki*= 31$\bar{4}$	*hki*= 42$\bar{6}$	*hki*= 61$\bar{7}$	*hki*= 53$\bar{8}$	*hki*= 64$\bar{10}$	*l*	*hki*= 41$\bar{5}$	*hki*= 52$\bar{7}$	*hki*= 71$\bar{8}$	*hki*= 63$\bar{9}$	*hki*= 82$\bar{10}$
														Intensity ×2. Average of ±*l*				
20	*a*	*a*	*a*	*a*	*a*	*a*	19	*a*	*a*	*a*	*a*	*a*	18	*a*	*a*	*a*	*a*	*vvw*
17	*a*	*vvw*	*a*	*a*	*a*	*a*	16	*a*	*a*	*a*	*a*	*a*	15	*vvw*	*a*	*a*	*a*	*a*
14	*a*	*a*	*a*	*a*	*w*	*a*	13	*a*	*m*	*a*	*a*	*a*	12	*vw*	*vvw*	*a*	*a*	*a*
11	*a*	*a*	*a*	*a*	*a*	*a*	10	*a*	*vw*	*a*	*a*	*vvw*	9	*a*	*a*	*a*	*a*	*vvw*
8	*a*	*a*	*a*	*a*	*a*	*a*	7	*a*	*vw*	*a*	*a*	*a*	6	*vw*	*vvw*	*a*	*a*	*a*
5	*vvw*	*vvw*	*a*	*a*	*w*	*a*	4	*a*	*s*	*a*	*a*	*vvw*	3	*vw*	*vvw*	*a*	*a*	*a*
2	*vvw*	*a*	*a*	*a*	*a*	*a*	1	*a*	*w*	*a*	*a*	*a*	0	*vvw*	*a*	*vvw*	*a*	*vvw*
$\bar{1}$	*vvw*	*vvw*	*a*	*a*	*a*	*a*	$\bar{2}$	*a*	*vw*	*a*	*a*	*a*						
$\bar{4}$	*m*	*a*	*a*	*a*	*w*	*a*	$\bar{5}$	*a*	*s*	*a*	*a*	*vvw*						
$\bar{7}$	*a*	*a*	*a*	*a*	*a*	*a*	$\bar{8}$	*a*	*w*	*a*	*a*	*a*						
$\bar{10}$	*vvw*	*a*	*a*	*a*	*a*	*a*	$\bar{11}$	*a*	*vw*	*a*	*a*	*vvw*						
$\bar{13}$	*vvw*	*a*	*a*	*a*	*vw*	*a*	$\bar{14}$	*a*	*m*	*a*	*a*	*a*						
$\bar{16}$	*a*	*a*	*a*	*a*	*a*	*a*	$\bar{17}$	*a*	*vvw*	*a*	*a*	*a*						
$\bar{19}$	*vvw*	*a*	*a*	*a*	*a*	*a*	$\bar{20}$	*a*	*a*	*a*	*a*	*a*						

* Average of ±*l*.

the presence of a centre of symmetry, may account for the lack of piezo-electric effect.

It is thus not possible to distinguish between the three crystal classes by external symmetry or piezo- and pyro-electric tests.

(d) Space-group considerations

For the hexagonal cell, $Z=9$. The cell therefore contains 9 Si + 27 Ca + 45 O. Calculated density = 3·21, observed = 3·12–3·25 g.cm.$^{-3}$. The diffraction symbol (Buerger, 1942, p. 511) is $\bar{3}mR$ −−. Possible space groups are $R\bar{3}m$, $R32$, $R3m$.

It is assumed that the Si^{4+} ion is tetrahedrally surrounded by four O^{2-} ions. Such tetrahedra cannot be placed at a symmetry centre or at the intersection of three- and twofold axes. They must, however, be in special positions in all three possible space groups, but only in $R3m$ can they be placed so as to account for the special features of the diffraction pattern listed above. This space group was therefore taken as the basis for a trial structure, with the SiO_4 groups and the nine other oxygen ions at (*a*) 0, 0, *z* for three different values of *z* in each case.

To produce the special features of the diffraction pattern and to satisfy packing considerations, the SiO_4 tetrahedra must be all pointing upwards with the silicon ions at 0, $\frac{2}{9}$, $\frac{7}{9}$ and with three non-tetrahedral oxygen ions between the SiO_4 groups at $\frac{2}{9}$ and $\frac{7}{9}$. This means that nine silicon ions and eighteen oxygen ions are on the trigonal axes, and the other twenty-seven oxygen ions are on the symmetry planes at (*b*) *x*, $\bar{x}$, *z*.

(e) Position of calcium

At this stage of the argument a rough model was made of the Si–O structure as deduced above. It was found that there were two sets of holes in which calcium ions could be placed. Only one set of positions satisfied Pauling's second rule even approximately, and only that set was consistent with the pseudo-halving of the *a* axis.

If the SiO_4 tetrahedra (which have two possible orientations at 60° to each other) are arranged with the basal oxygen ions directly above the calcium ions, Pauling's rule is obeyed exactly, and this arrangement was therefore taken as the basis for a trial structure. In this arrangement the bases of the SiO_4 tetrahedra at $z=0$ and $\frac{7}{9}$ point in the direction [1$\bar{1}$.0] that at $z=\frac{2}{9}$ in the opposite direction.

These considerations give rough co-ordinates for the various atoms. It remains to use packing data to calculate more exact co-ordinates.

(f) The derivation of co-ordinates from packing data

Taking the O–O distance in the SiO_4 tetrahedra as 2·6 Å (Bragg, 1937, p. 20) and 2·7 Å as the diameter of the single oxygen ions, it can be shown (Jeffery, 1950) that the silicon and oxygen positions are determined. The 'holes' left for the calcium ions, which are 6 co-ordinated, are then almost exactly the right size, assuming the radii of calcium and oxygen ions to be 0·99 and 1·35 Å respectively. There are three cases. In case (1) the calcium is 'loose' with a range of movement of 0·1 Å from the mean position and with one oxygen ion leaving a gap of 0·2 Å. In cases (2) and (3) the calcium ion is touched by five oxygen ions, and one oxygen ion leaves a gap of 0·15 and 0·1 Å respectively. However, the arrangement of the oxygen ions is almost exactly the same in each case and is shown in Fig. 9. There are thus ten Ca–O bonds of length 2·34, six of length 2·44, one of length 2·49 and one of length 2·54 Å.

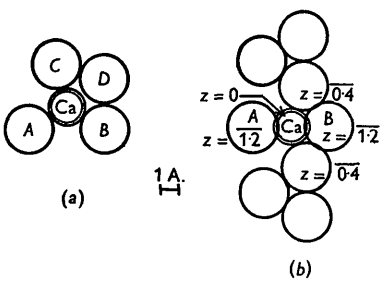

Fig. 9. Diagrams showing the surroundings of calcium atoms. (*a*) Section in the plane of symmetry. (*b*) Plan (atoms *C* and *D* not shown).

(g) The effect of changing the orientation of the SiO_4 *tetrahedra*

If any of the three independent SiO_4 tetrahedra are given the alternative orientations, the structure still packs in an almost exactly equivalent fashion as regards the silicon and oxygen ions, with negligible changes in the *z* co-ordinates of all the atoms. However, for each such change in orientation a calcium ion becomes 7 co-ordinated, with two oxygen ions at 2·92 Å instead of one at 2·34 Å. In Fig. 9 (*a*), *C*, which is one of the base oxygen ions of a tetrahedron (shown in relation to the axes in Fig. 13), is swung round until two of the base oxygen ions are equidistant from the calcium ion. There is no change in the position of any of the other oxygen ions co-ordinating that calcium ion. But if the first alteration is to Ca (2) (Fig. 13), Ca (3) has the arrangement represented in Fig. 9 (*b*) turned into its mirror image. If any such alteration is made, Pauling's rule is no longer exactly obeyed.

(h) The atomic co-ordinates of the trial structure

The fractional co-ordinates for all the independent atoms are given in Table 2.

(i) Comparison of observed and calculated structure factors

The intensities were measured from the photographic film by eye-estimation against a standard scale and were corrected for the Lorentz and polarization factors, using the scale described by Goldschmidt & Pitt (1948). The square roots of the corrected values were multiplied by a normalizing factor which made $\overline{F}_o = \overline{F}_c$.

The calculated *F* values were obtained from the atomic co-ordinates (Table 2) and the *f* values given by Bragg & West (1928), which are empirically corrected for heat motion. The simple calculating machine described by Booth (1947) was used for the evaluation.

Fig. 10 shows graphically the comparison between the observed and calculated *F* values for the three zones *hki*0, $hh.2\bar{h}l$ and $h0\bar{h}l$. The general agreement is as good as can be expected from a pseudo-structure, and demonstrates that the distortion of this structure must be small.

(j) Conclusions

It can be concluded that the actual positions of calcium and silicon in the structure must be very near to those given by the assumed co-ordinates, and that the oxygen positions on the trigonal axes are also approximately correct. However, the orientations of the SiO_4 tetrahedra are not necessarily correct. A change of orientation does not affect the $hh.2\bar{h}l$ reflexions. In the *hki*0 zone only $30\bar{3}0$ is appreciably affected by such a change. In the $h0\bar{h}l$ zone thirteen reflexions, showing the worst agreement, were selected, and *F* values were calculated for all the eight possible combinations of SiO_4 orientation. This was also done for $30\bar{3}0$, in which most of the contribution to the *F* value is from the tetrahedral oxygen ions.

Fig. 11 gives these results in graphical form, and it is evident from this, and also from an elementary statistical analysis, that no combination gives significantly better agreement than any other. This means that the errors in the assumed co-ordinates, including the errors involved in the use of a structure-factor expression which implies trigonal symmetry, are of the same order as those arising from an incorrect orientation of the SiO_4 tetrahedra. However, rather more significance attaches to the case of $30\bar{3}0$, since the *z* co-ordinates do not enter into the calculated *F* values. In this case those combinations which have one independent tetrahedron orientated differently from the other two give much better agreement with the observed value than when all three are orientated in the same way. The orientation assumed in the trial structure gives rather better agreement than its alternative, but this difference is probably not significant.

Table 2. *Atomic co-ordinates*

	Si (1)	Si (2)	Si (3)	O (1)	O (2)	O (3)	O (4)	O (5)	O (6)	O (7)	O (8)	O (9)	Ca (1)	Ca (2)	Ca (3)
x	0	0	0	0	0	0	0	0	0	0·124	0·876	0·124	0·495	0·835	0·505
z	0	0·226	0·783	0·064	0·290	0·847	0·398	0·506	0·614	0·980	0·206	0·763	0·003	0·112	0·224

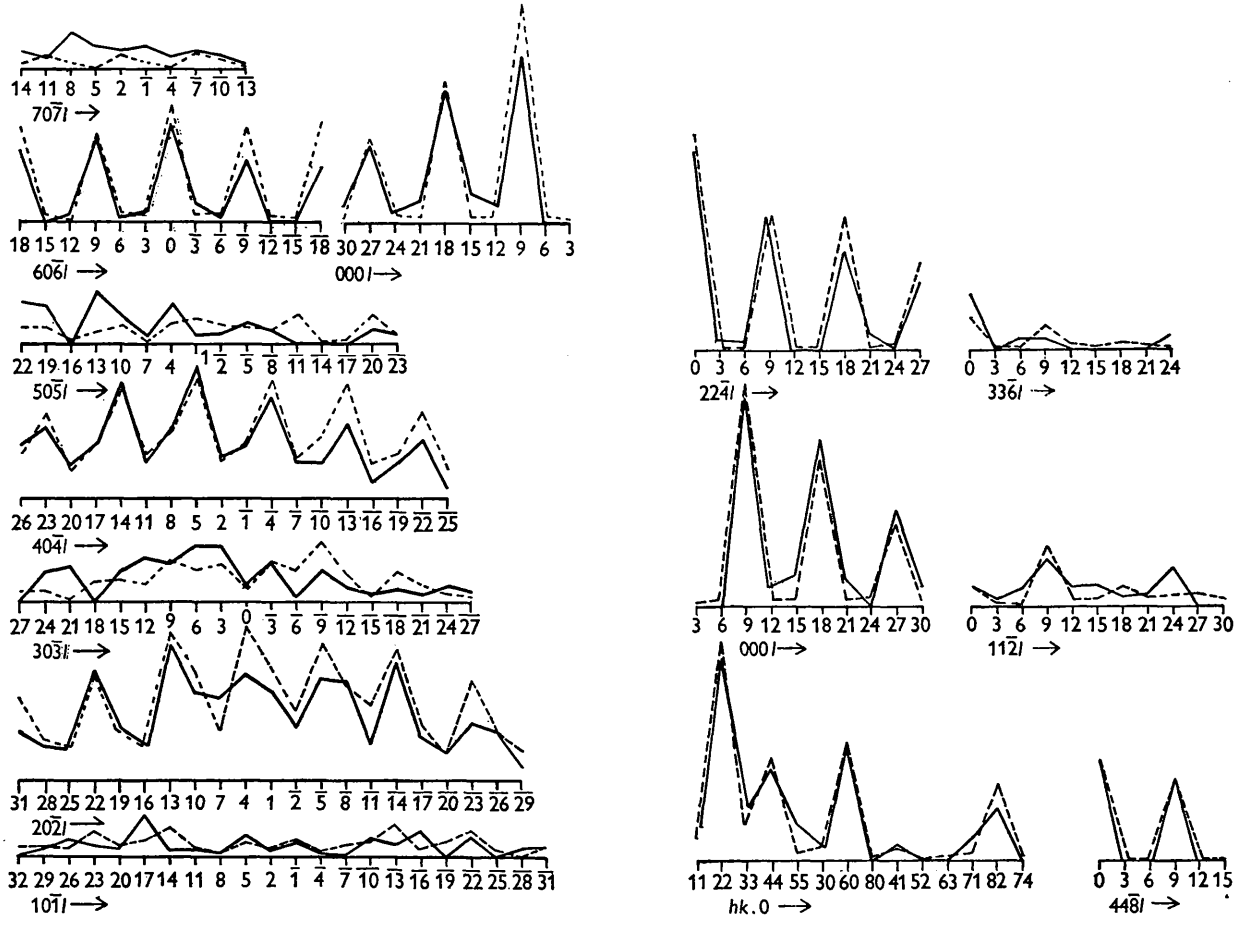

Fig. 10. Comparison of observed (full lines) and calculated (broken lines) F values.

If the three tetrahedra are not all orientated in the same way, it is very probable that the trial structure is correct, since it has the lowest energy of the six possible combinations which have two groups in one orientation and the third in the other. It also has much better packing of the oxygen ions co-ordinating the calcium. More complete confirmation of this, however, together with any further refinement of the atomic co-ordinates, must wait until the true structure is worked out in detail, using a structure-factor expression based on the true symmetry.

Figs. 9, 12 and 13 show the idealized or pseudo-structure arrived at in this way.

Other recent work on the structure of tricalcium silicate

After the presentation of the thesis (May, 1950), part of which has been given in an abridged and amended form in this paper, a note on the structure of tricalcium silicate was received from Prof. O'Daniel (O'Daniel & Hellner, 1950). This is a preliminary account of work done at the Kaiser Wilhelm Institute at the beginning of the war, and the structure deduced differs considerably from that given in the present paper. The trial structure was obtained from the CaO structure by replacing three out of four calcium ions in every third layer by oxygen and shifting adjacent

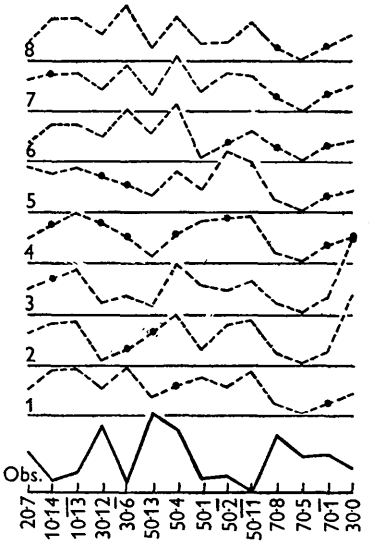

Fig. 11. Comparison of observed and calculated F values for fourteen selected reflexions and the eight possible combinations of SiO_4 orientation.

layers to give tetrahedral holes into which the silicon ions fit. This gives Si_3O_9 rings and concentrates the silicon ions into three layers in the hexagonal cell, instead of nine as in the structure given here. The

As no comparison of observed and calculated structure factors is given beyond the general statement that agreement is 'good', it is difficult to assess the significance of the proposed structure. Calculation

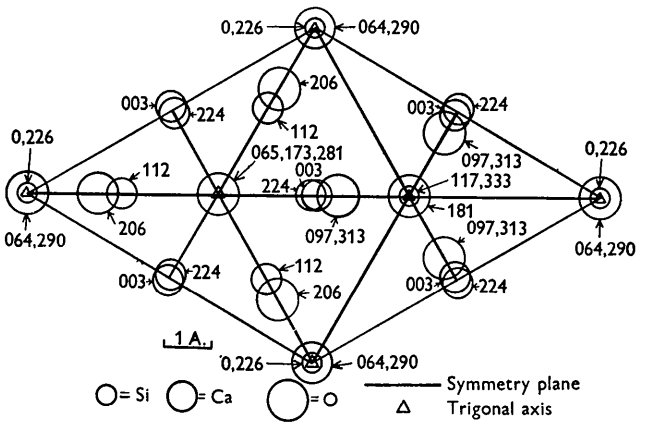

Fig. 12. Diagram of the bottom layer of the idealized or pseudo-structure. The second and third layers are identical but displaced by one-third of the lattice spacing in the direction of [1$\bar{1}$.0]. The figures are thousandths of the cell height.

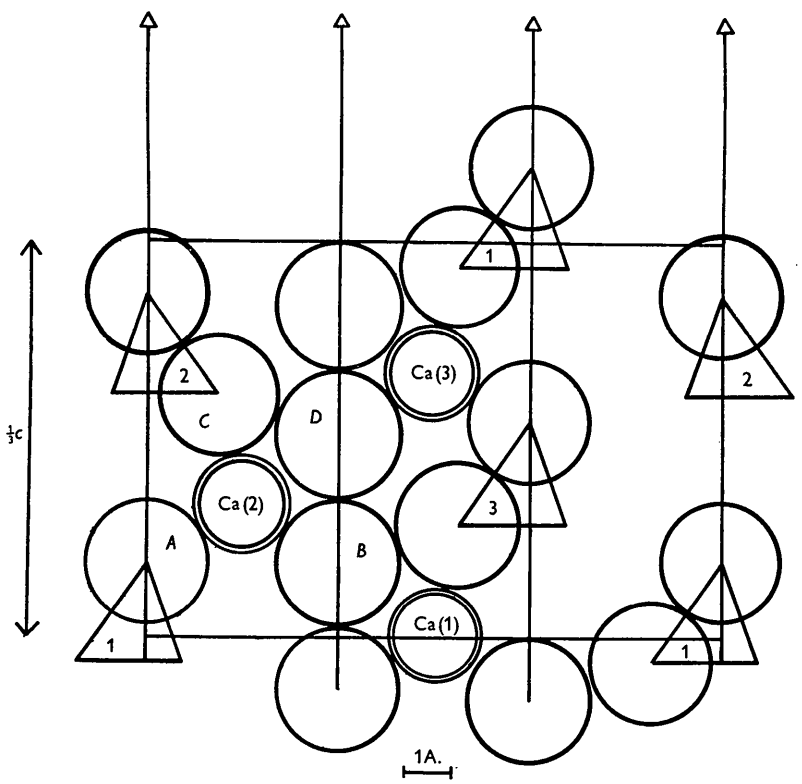

Fig. 13. Vertical section of the bottom layer of the pseudo-structure through the long diagonal of the cell. Only the oxygen atoms in the symmetry plane are shown.

rings seem improbable on chemical grounds, since tricalcium silicate breaks down on slow cooling between 1250 and 600° C. into β dicalcium silicate and lime, and the β dicalcium silicate transforms into γ dicalcium silicate,. which has an olivine structure (O'Daniel, 1941) with separate SiO_4 tetrahedra. It seems unlikely that rings would break down under these circumstances.

from the co-ordinates given in the paper shows that, because of the near equivalence in scattering power of (Si + O) and Ca, the $000l$ and $60\bar{6}l$ reflexions (two of the most characteristic row lines) do not provide adequate means of deciding between the two structures. The agreement given by the structure above is better than that obtained from the co-ordinates given by O'Daniel

& Hellner, but it will be necessary to await the full paper, which is promised, before an adequate comparison can be made.

The Si–O bond lengths derived from these co-ordinates seem to be rather unusual, but as some correction to the co-ordinates in the full paper is foreshadowed, it will again be best to wait for its appearance before attempting any comparison.

A point on which it is possible to be rather more definite concerns the symmetry of tricalcium silicate. O'Daniel & Hellner conclude that the evidence already given (Jeffery, 1949) for departure from trigonality is due to missetting and twinning. The possibility of twinning is, however, excluded by the successful indexing (see later) of the 'extra' reflexions. The setting for every Laue photograph reproduced in this paper has been checked and is correct to 0·05°, showing that no appreciable missetting has occurred.

The investigation of the monoclinic lattice of alite

(*a*) *General*

It has been shown above that alite has a pseudo-rhombohedral structure, but that its true symmetry (with certain reservations to be discussed later) is monoclinic.

The first suspicions that the rhombohedral cell might only be a pseudo one were aroused by the presence on the rotation photograph of four spots surrounding the extremely strong reflexion $22\bar{4}0$, and not lying on the rhombohedral layer lines. It was, however, not until the large alite crystal was available that the significance of these 'satellite' spots could be determined. The rotation photograph of the recrystallized alite crystal (Fig. 1) shows exactly the same main pattern as that of the clinker crystal, but besides the four spots surrounding $22\bar{4}0$ it shows a large number of other 'satellite' spots. (It was already known from oscillation photographs that the reciprocal-lattice points associated with the four spots surrounding $22\bar{4}0$ were very close to the $22\bar{4}0$ reciprocal-lattice point, and it appeared probable from the rotation photograph that this was the case for other spots. Hence the name 'satellite'.) These 'satellite' spots must correspond to the monoclinic unit cell, which will be a multiple of the pseudo cell. However, because of this 'satellite' character of reflexions from the monoclinic lattice other than those corresponding to the pseudo cell, it is difficult even to establish the monoclinic cell dimensions. The monoclinic reciprocal-lattice points cannot be detected over large regions of Fourier space, and thus the relation between the various sets of 'satellite' points is difficult to determine.

(*b*) *Experimental data on the true lattice*

The following results are given in the order in which they were obtained. All photographs were heavily exposed to bring up the weak reflexions. Cu $K\alpha$ radiation was used throughout.

(i) Rotation photograph about the hexagonal c axis (Fig. 1). The ζ and ξ values for a considerable number of 'satellite' spots on this photograph were measured, using a Bernal chart. In all cases, to within the error of measurement, the spots lay at one-sixth of the rhombohedral layer-line spacing above or below the main layer lines. This would give a crystal-lattice spacing in the c direction of about 150 Å.

A further feature of the satellite spots is that they occur on row lines with three sequences of distribution. If we make one-sixth of the rhombohedral layer-line spacing the unit for ζ measurement, the ζ values of the first sequence are: 7, 47, 61; of the second: 1, 17, 37, 53, 55; and of the third: 5, 13, 23, 31, 41, 67. On most row lines only parts of the sequences were present, particularly in the second and third cases, and in a few instances the ξ values of the row lines were so nearly equal that it was difficult to separate them. Nevertheless, it was possible to measure eight examples of the first sequence, five of the second and four of the third.

(ii) Rotation photograph about that hexagonal a^* direction [21.0], which lies in the true reflexion plane (Fig. 7). Here the layer-line spacing is one-third of that for the rhombohedral lattice.

(iii) Rotation photograph about that hexagonal a axis [01.0], which is perpendicular to the true reflexion plane (the monoclinic b axis) (Fig. 8). The layer-line spacing is the same as for the rhombohedral lattice.

(iv) Equi-inclination Weissenberg photographs, about the b axis, of the zero, first and second layers. The zero-layer photograph includes the whole reciprocal net within the limiting sphere. The first-layer photograph had an oscillation of 30°, designed so that the only strong reflexion in this layer came in the middle of the oscillation. The second-layer photograph had an oscillation of 60° and included about two-thirds of the reciprocal net within the limiting sphere. All three photographs show the presence of 'satellite' spots, usually a pair, one on either side of the main reflexion, sometimes two on one side and one on the other, more rarely a second pair nearly at right angles to the first and always very weak.

(*c*) *Interpretation of the experimental data*

The distances between the inner $44\bar{8}0$ α_1 reflexions on the hexagonal c-rotation photograph and between the 0.0.0.27 and 0.0.0.30 pairs of α_1 reflexions on the hexagonal a^*-rotation photograph were measured on a travelling microscope and converted to ξ values. The ξ value for $44\bar{8}0$ gave $8b^*$ for the monoclinic lattice directly. The value of hexagonal a^* in the reflexion plane was calculated from $\xi_{44\bar{8}0}$. The indexing of 0.0.0.30 was checked against the strong reflexion 0.0.0.27 and then the ξ value was used to obtain hexagonal c^*. The rhombohedral a^*c^* net perpendicular to monoclinic b was then drawn out accurately, and the 'satellite' spots from the zero-layer Weissenberg photograph were plotted out from the main reflexions, using

a Weissenberg reciprocal-co-ordinate chart. This was repeated for the first-layer photograph. The result is shown in Fig. 14. All the points lie on the new reciprocal net drawn on the diagram. The satellite spots of the second layer could almost all be assigned reciprocal-lattice points corresponding to this zero-layer net (the few exceptions are discussed in the next section). The first-layer points of the rhombohedral lattice (only one of which is shown in Fig. 14) are in body centring positions relative to the zero- and second-layer rhombohedral nets, but both these points and their satellites are in face-centring positions

65; 5, 13, 23, 31, 41, 49, 59, 67. This accounts for the measured values of ζ for different row lines given in § (*b*) (i).

The rows of reciprocal-lattice points parallel to hexagonal c^*, mentioned above, account for some of the layer lines (nos. 1, 5, 7, etc.) in the rotation photograph about a^* (§ (*b*) (ii)) which give the thirding of the rhombohedral layer-line spacing. To account for the others (nos. 2, 4, 8, 10, etc.) we cannot make use of the 'satellite' points of the first layer of Fig. 14, since hardly any occur with detectable weight. But sufficient reflexions occur corresponding to the second line

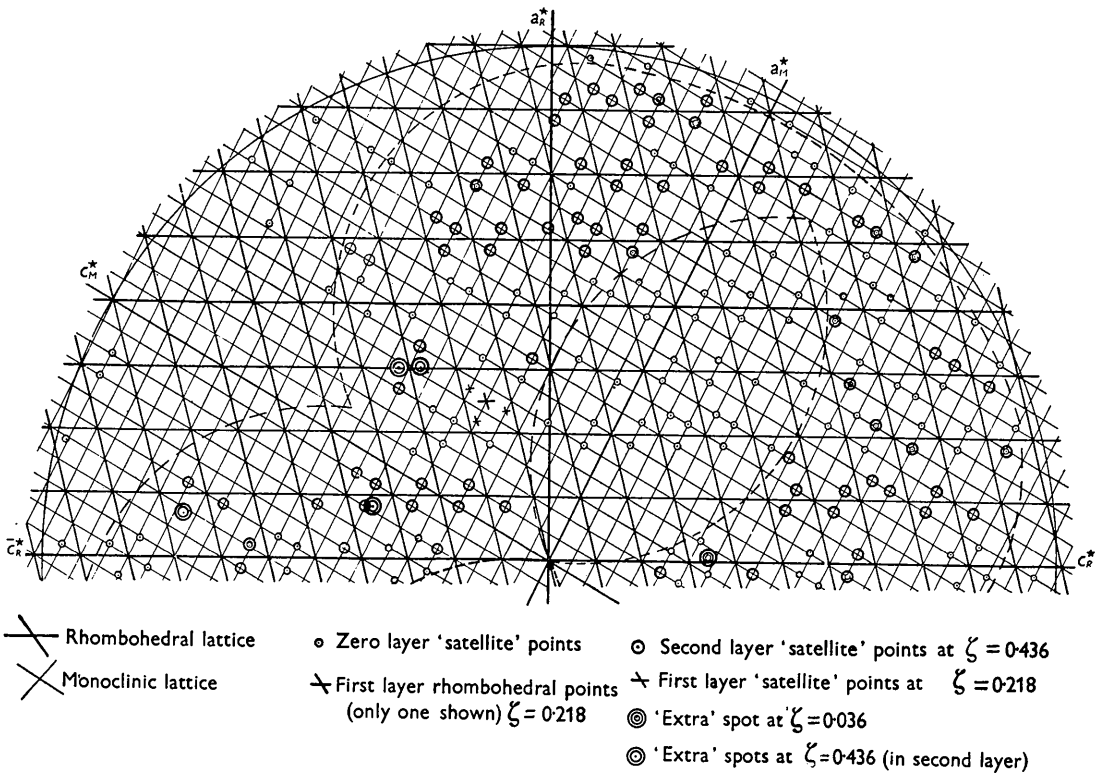

Fig. 14. The reciprocal-lattice net showing the results of interpreting the zero-, first- and second-layer Weissenberg photographs about the monoclinic *b* axis. (The second-layer oscillation covered the area between the inner and outer broken curves.)

relative to the zero- and second-layer monoclinic nets. The directions chosen for the axes make the monoclinic unit cell *C*-face centred.

The monoclinic a^*, c^* and β^* were calculated from the hexagonal a^* and c^* values, and, together with b^* obtained above, lead to the following monoclinic cell dimensions:

$$a = 33{\cdot}08, \quad b = 7{\cdot}07, \quad c = 18{\cdot}56 \text{ Å}, \quad \beta = 94° 10'.$$

This lattice accounts for the main features of the three rotation photographs listed above. In particular, if we take the monoclinic lattice points on either side of the rhombohedral row lines parallel to hexagonal c^* (Fig. 14), we get the following three sequences of ζ values for the row lines of a rotation photograph about this axis: 1, 17, 19, 35, 37, 53, 55; 7, 11, 25, 29, 43, 47, 61, of monoclinic points away from the rhombohedral row lines, in the zero and second layers of Fig. 14, to account for the corresponding layer lines in the a^* rotation photograph.

(*d*) *Exceptions to the interpretation given in* § (*c*)

(i) A close inspection of the symmetrical Laue photograph (Fig. 5) shows a few spots without reflected counterparts. It is possible that such spots were produced by the characteristic component of the radiation, and that because of the slight missetting (*c.* 0·05°) the symmetrically related planes reflected only a very much weaker component of the white radiation. It seems probable, however, from the evidence of the rotation and Weissenberg photographs,

that they may represent a slight departure of the structure from monoclinic symmetry.

(ii) The rotation photograph about the hexagonal a^* axis (Fig. 7) shows not only layer lines at one-third the distance of the rhombohedral layers, but also a few spots half-way between these monoclinic layers. These spots are not accounted for by the cell given above.

(iii) The rotation photograph about b (Fig. 8) shows faint layer lines at one-sixth of the main spacing above and below the main lines. (This photograph was very heavily exposed, and a considerable number of β spots show up strongly in spite of the filter. The β-layer line and one of the 'satellite' layers are nearly coincident for the second main layer, but are more separated for higher layers.) It has been possible to locate definitely only one of these points, which lies near 0009, and is the only one with an intensity comparable with those of the monoclinic 'satellite' spots. This point was located from the two rotation photographs, and also from a Weissenberg photograph taken with one side of the slit in the layer-line screen opened to take in the 'satellite' layer as well as the zero layer. This point is marked on Fig. 14. A 5°-oscillation Weissenberg photograph arranged to take in both satellite layers as well as the zero layer showed that these 'extra' spots do not show monoclinic symmetry.

(iv) The Weissenberg second-layer photograph shows four spots which do not fit the reciprocal net given above. They are all among the weakest of the 'satellite' spots.

(v) It has not been possible to determine the lattice on which these 'extra' reciprocal points lie, except that some of them lie half-way between the monoclinic layers perpendicular to hexagonal a^* and at one-sixth the interval between the layers perpendicular to b. The unit cell must therefore be at least six times as large as the monoclinic cell. It is almost certain that the larger cell is triclinic. Since all but one of these 'extra' reflexions are, in practice, too weak to have their reciprocal-lattice points located, it is clear that the distortion of the monoclinic structure must be very small. But it is noteworthy that such small distortions, repeating over distances of 40 Å or more, should be sufficiently regular to give sharp reflexions.

(e) *The monoclinic space group*

The monoclinic lattice can have the symmetry only of one of the subgroups of $R3m$, and the space group must therefore be Cm.

(f) *The relation between the rhombohedral and monoclinic crystal lattices, and the distortion of the rhombohedral lattice*

Fig. 15 shows this relationship for the zero and first layers of both lattices. The b spacing, perpendicular to the paper, is the same for both lattices. The rhombohedral lattice angles are not distorted by more than 2–3′.

(g) *The monoclinic cell contents*

A simple calculation from the chemical analysis shows that there is approximately one molecule of Al_2O_3 and one of MgO in the asymmetric unit of the monoclinic cell. The monoclinic cell is twelve times the volume of the primitive rhombohedral cell, and is face-centred. If the chemical formula were $3CaO.SiO_2$, the monoclinic asymmetric unit would contain

$$54\,CaO + 18\,SiO_2.$$

If we suppose that 2 Al replace 2 Si, and that 1 Mg comes into a nearby hole to balance the charges, we get $54\,CaO + 16\,SiO_2 + Al_2O_3 + MgO$ as the contents of the asymmetric unit. If now we replace Al_2O_3 by Fe_2O_3 to the extent indicated by the chemical analysis, and do the same with MgO and FeO, we obtain a percentage composition which is the same as that given by the analysis to within the experimental error.

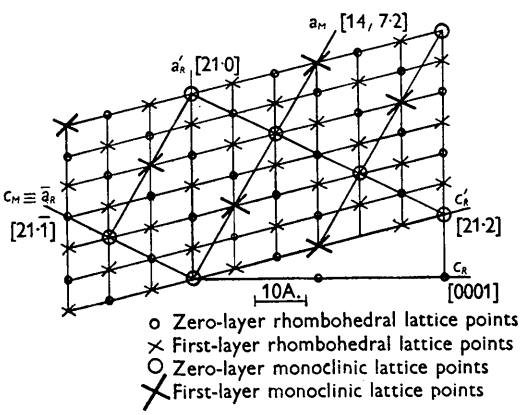

Fig. 15. The relationship between the rhombohedral and monoclinic crystal lattices. c_R is the c axis when the rhombohedral lattice is referred to hexagonal axes. a'_R and c'_R are the crystal axes, defining an all-face-centred lattice, corresponding to the body-centred orientation of the rhombohedral reciprocal lattice given in Fig. 14. $\bar{a}_R$ is the negative direction of one of the crystal axes of the primitive rhombohedral cell. a_M and c_M are the monoclinic crystal axes. The co-ordinate directions refer to the hexagonal axes.

The density calculated from the above cell contents is 3·227 g.cm.$^{-3}$. The measured density varies from 3·14 to 3·25 g.cm.$^{-3}$. This variation, while making no difference to the calculated number of molecules of Al_2O_3, MgO and SiO_2 in the asymmetric unit, can lead to a reduction of two in the number of molecules of CaO if a density of 3·13 is taken instead of 3·23 g.cm.$^{-3}$. It is thus desirable that the true density should be further investigated.

(h) *Possible arrangement of atoms in the monoclinic cell*

The magnesium must be on the symmetry plane in the space group Cm. The two oxygen tetrahedra in which Al is substituted for Si must lie either one on each side of the symmetry plane or both in the symmetry plane. It can be shown (Jeffery, 1950) that they are almost certainly in the symmetry plane, and that the most probable co-ordinates in the rhombohedral

pseudo-cell, consistent with the previous derivation of the monoclinic cell, are $\frac{5}{3}$, $\frac{5}{6}$, $\frac{1}{9}$ approximately. The aluminium positions are $\frac{4}{3}$, $\frac{2}{3}$, $\frac{1}{9}$ and 2, 1, $\frac{2}{9}$.

On Fig. 12, which assumes trigonal symmetry, the equivalent positions are Mg: $\frac{1}{6}$, $\frac{5}{6}$, $\frac{1}{9}$; Al: $\frac{1}{3}$, $\frac{2}{3}$, $\frac{1}{9}$ and 0, 1, $\frac{2}{9}$. Fig. 16 shows the probable form of the distortion caused by the substitution. Until detailed analysis based on the monoclinic cell is undertaken this is the most that can be deduced about the magnesium and aluminium positions.

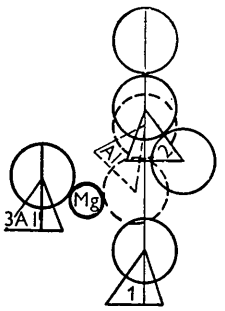

Fig. 16. Possible arrangement of Mg and two AlO_4 tetrahedra, showing the main distortion produced in the rhombohedral structure. The undistorted arrangement shown is the same as the right-hand bottom corner of Fig. 13 and, as in that case, the tetrahedral oxygen atoms above and below the plane of the paper are omitted.

(i) Deductions from the intensities and positions of the 'satellite' monoclinic reflexions

The weakest observable pseudo-rhombohedral reflexions have an F value (calculated for the monoclinic cell) of about 120. If we suppose the rhombohedral lattice to be undistorted, and neglect the effect of the substitution of four silicon ions by aluminium, then the only contribution to the satellite reflexions would come from the two magnesium ions. This would give an F value of 20 for the zero-order satellites, and the value for other satellites would decline with increasing θ according to the atomic scattering curve for magnesium. Thus all the satellite spots would be unobservable. The observed reflexions must therefore be mainly due, not to periodic variations of density caused by substitution, but to a periodic distortion of the rhombohedral lattice. This is confirmed by the fact that the zero-order satellites cannot be detected, and that the relative intensity of the satellites increases with increasing order. This is precisely the effect to be expected from such a lattice distortion (James, 1948, p. 563). Since almost all the satellite reciprocal-lattice points occur on either side of a heavily weighted rhombohedral point in the direction of the monoclinic c^* axis, the distortion of the rhombohedral lattice, to a first approximation, takes place by a displacement of the planes (001) (monoclinic) or $(20\bar{2}7)$ (hexagonal) along their normal. The direction of displacement is very nearly along one of the rhombohedral axes, and the period very nearly twice the length of that axis, i.e. approximately 19 Å. A maximum displacement of *c.* 0·1 Å would account for the observed effects (James, 1948, p. 563).

The role of the Al and Mg which replace Si is thus to act as a kind of 'organizing centre' to produce a symmetrical distortion in a structure which cannot quite adopt a stable rhombohedral configuration. Without this 'organizing centre' an unsymmetrical and possibly less stable distortion takes place, and the triclinic structure of pure tricalcium silicate results.

It is probable that other, much smaller, distortions are present in the structure, and give rise to the reflexions which cannot be accounted for by the monoclinic lattice. These may be connected with the replacement of aluminium by iron, but the information available is insufficient even to indicate how this substitution might take place, except to show that it occurs with a considerable degree of regularity. Work on lamellar structure and superlattice effects in the potash–soda and plagioclase felspars has shown that so-called solid solution is often accompanied by a regular arrangement of atoms with large repeat distances (Taylor, Chao & Smare, 1939; Taylor & Chao, 1940).

The author wishes to thank Prof. J. D. Bernal for his constant encouragement and advice and Dr F. M. Lea, Director of the Building Research Station, for permission to publish this work, which was carried out as part of a programme of extra-mural research for the Building Research Board.

References

ANDERSEN, O. & LEE, H. C. (1933). *J. Wash. Acad. Sci.* **23**, 338.
BOOTH, A. D. (1947). *J. Appl. Phys.* **18**, 664.
BRAGG, W. L. (1937). *The Atomic Structure of Minerals.* Ithaca: Cornell University Press.
BRAGG, W. L. & WEST, J. (1928). *Z. Krystallogr.* **69**, 118.
BUERGER, M. J. (1942). *X-ray Crystallography.* New York: Wiley.
GOLDSCHMIDT, G. H. & PITT, G. J. (1948). *J. Sci. Instrum. Phys. Ind.* **25**, 397.
GUTTMANN, A. & GILLE, F. (1933*a*). *Zement*, **22**, 383.
GUTTMANN, A. & GILLE, F. (1933*b*). *Zement*, **22**, 402.
JAMES, R. W. (1948). *The Optical Principles of the Diffraction of X-Rays.* London: Bell.
JEFFERY, J. W. (1949). *Mag. Concrete Res.* **2**, 99.
JEFFERY, J. W. (1950). Ph.D. Thesis, London University.
NURSE, R. W. (1949). *J. Sci. Instrum. Phys. Ind.* **26**, 102.
O'DANIEL, H. (1941). *Zement*, **40**, 1.
O'DANIEL, H. & HELLNER, E. (1950). *Neues Jb. Min. Geol. Paläont.* **5**, 108.
TAYLOR, W. H., CHAO, S. H. & SMARE, D. L. (1939). *Miner. Mag.* **25**, 338.
TAYLOR, W. H. & CHAO, S. H. (1940). *Proc. Roy. Soc.* A, **176**, 76.
WOOSTER, W. A. (1949). *A Text Book on Crystal Physics.* Cambridge University Press.